

Inlet Drag and Stability Considerations for $M_0 = 2.00$ Design

R. H. Tindell*

Grumman Aerospace Corporation, Bethpage, N.Y.

The results of an experimental study to evaluate the performance and low-flow stability limits of several isolated inlet models are presented. The lowest drag approach to provide large-flow regulation was a bypass device for handling the excess airflow. The use of compression surface modulation or a boundary-layer bleed system to dispose of the excess airflow incurred similar drag penalties which were significantly greater than those for the bypass configuration. A good correlation of low-flow stability range data with a shock-lip geometry parameter is demonstrated. A by-product of this work is the introduction of a drag parameter that allows a more complete approach to quantifying inlet drag characteristics.

Nomenclature

A	= area
C_D	= drag coefficient ($D/q_0 A_c$)
H	= throat height
L	= distance between lip and normal shock position for slipstream ingestion
P	= pressure
W_c	= corrected weight flow
α, β	= lip angles
δ	= compression surface turning angle
ϕ	= angle between lip and leading edge of the shock-generating surface
θ	= discharge angle

Subscripts

0	= freestream
2	= engine face
B	= bleed exit
c	= capture
e	= bypass exit
T	= total and throat

Introduction

THE proposed requirements of supersonic aircraft during the period of the mid-1980s to the 1990s are expected to be considerably more demanding on both airframe and engine manufacturers than those reflected in current aircraft mission capabilities. Requirements for future systems include supersonic cruise in the Mach 1.6-2.0 range for sustained time periods much greater than current capabilities. In order to meet these requirements, inlet pressure recovery and drag must be optimized concurrently with an adequate inlet airflow stability range. Unfortunately, low inlet drag and a large stable airflow range for multishock inlets tend to be competing factors.

Studies describing various aspects of this design problem have been made previously; however, no consistent set of data that reflects the effects of a broad spectrum of inlet design elements (such as bypass systems, bleed systems, etc.) is available. The primary aim of this paper is to define such a set of wind-tunnel model data, with appropriate analysis, that can be used to establish the tradeoffs between inlet performance and low-flow stability.

Presented as Paper 80-1105 at the AIAA/SAE/ASME 16th Joint Propulsion Conference, Hartford, Conn., June 30-July 2, 1980; submitted Aug. 22, 1980; revision received March 12, 1981. Copyright © American Institute of Aeronautics and Astronautics, Inc., 1980. All rights reserved.

*Head, Propulsion Fluid Mechanics Group.

The approach taken here is to alter incrementally the inlet compression system from a simple normal shock configuration to a multishock design and to evaluate the benefits and problems associated with high-performance designs. This approach not only allows a clear insight into the integration of the various elements of the inlet design, but also provides an opportunity to define a more complete inlet drag bookkeeping system.

Figure 1 shows how the excellent stability of a low-drag normal shock inlet is compromised in a greater pressure recovery multishock inlet. The gap between the oblique shock and the cowl lip, which is required to allow the normal shock to move forward as engine airflow is reduced, causes an oblique shock spillage drag penalty at maximum airflow operating conditions. As the engine airflow is reduced, the static pressures in the diffusing inflow increase until the local total pressure is exceeded. Then, local reverse flow and separation occur, leading to flow blockage, unstable flow, and buzz. This criterion for inlet stability is discussed in Ref. 1. The buzz margin shown in Fig. 1 is discussed extensively in this reference. It is the difference between the maximum matched-engine corrected weight flow and the corrected weight flow at the incipient buzz point, divided by the maximum matched flow.

Figure 2 shows two areas where reverse flow and separation occur. The low boundary-layer total pressure near the compression surface is one area of concern, and the low total pressure on the merged shock side of the triple point (shock intersection) is another. There is diffusion downstream of both areas, with the potential for instability as engine airflow is reduced. Control of the compression surface boundary layer, either by removing it or by energizing it, can significantly improve the low-flow stability picture. The shock-lip diffusion situation must also be carefully monitored in the process of establishing an optimum performance vs stability tradeoff.

There must be enough stable inlet operating range to allow buzz-free operation for engine airflows from maximum power down to idle. This range can be up to 20-30% of the maximum airflow. If the additional requirement to provide buzz-free operation under engine stall conditions is imposed to allow for smooth engine recovery, the required stable airflow range can be as large as 50% of the maximum engine airflow. Therefore, proper tradeoffs must be made between satisfactory inlet performance and stable airflow operating range, i.e., buzz margin.

A step toward defining these requirements was made during an experimental evaluation of isolated external compression inlet configurations in a blowdown wind tunnel at $M_0 = 2.00$. The primary goal of the test was to determine the major effects of the compression system shock structure, cowl lip geometry, boundary-layer bleed system, and airflow matching technique upon the inlet drag and stability characteristics.

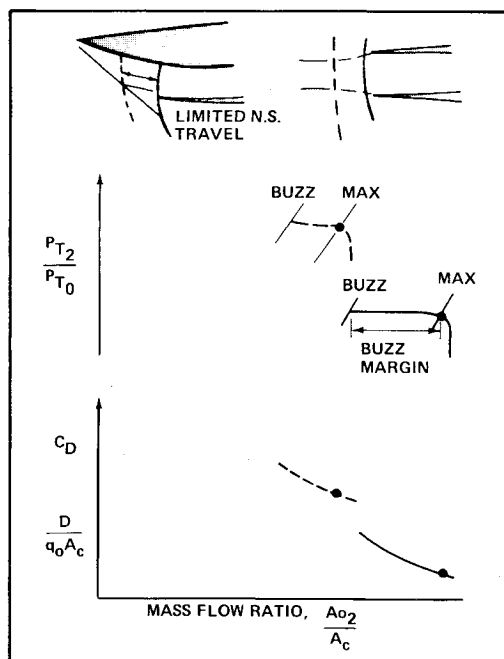


Fig. 1 Inlet characteristics.

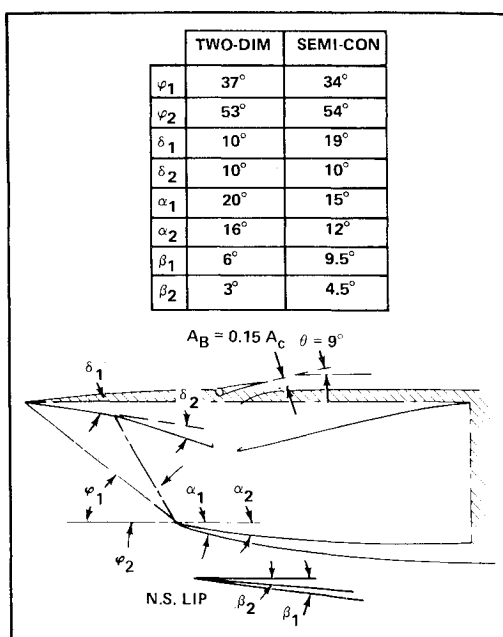


Fig. 4 Baseline inlet model configurations.

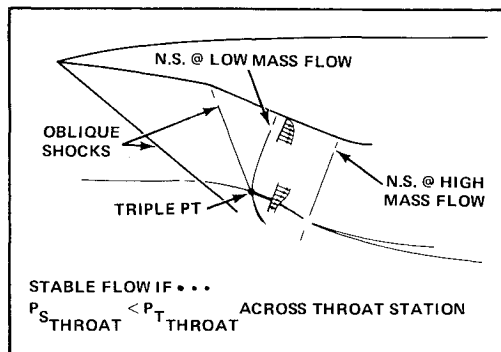


Fig. 2 Stability considerations.

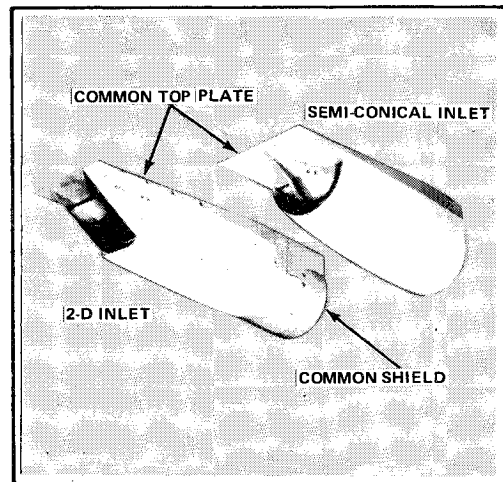


Fig. 5 Isolated models.

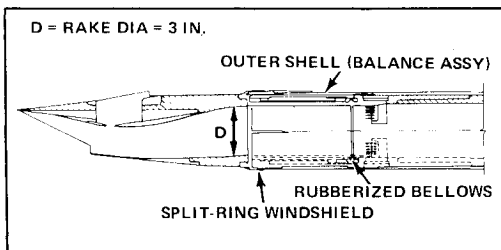


Fig. 3 Inlet model—balance assembly.

Apparatus

Model and Total Pressure Rake

Two modular inlet models were designed for evaluation in the Grumman 15 × 15 in. supersonic blowdown wind tunnel. The models are a square two-dimensional isolated inlet and a semiconical inlet of equal length, both with a 7 in.² capture area. Figure 3 shows the two-dimensional model assembly. It mounts to a three-component cylindrical flow-through balance, and is isolated from its nonmetric support tube by a rubberized bellows system. The inlet duct, from total pressure rake face to cowl lip, is six rake diameters long. The internal diffusion section is three rake diameters long, within which the duct shape changes into a circular section. The remaining

duct length of three diameters is a constant area section and is common to both the two-dimensional and semiconical inlets. The total pressure probes at the rake station are arranged in eight symmetrical rays, each containing five probes. This 40-probe rake is located just upstream of the internal metric-nonmetric break and includes only low-response (steady-state) transducers. A mass flow control plug valve is located downstream of the rake.

The inlet compression ramps, cowl lips, and inlet ramp bleed exits are all readily changeable, providing an array of combinations for testing and evaluation. The angle of attack was maintained at 0 deg throughout the test.

Compression System

The baseline configurations for both inlets are three-shock systems having approximately the same pressure recovery (see Figs. 4 and 5). All nonvariable model elements are identical on both inlets, so a direct drag comparison can be made.

The duct entrance area between the ramp (or cone) surface and the lip leading edge does not contract beyond the local design Mach number's A/A^* ratio. The internal lip angles are 16 and 12 deg for the two-dimensional and the semiconical configurations, respectively. The corresponding external cowl angles are 20 and 15 deg.

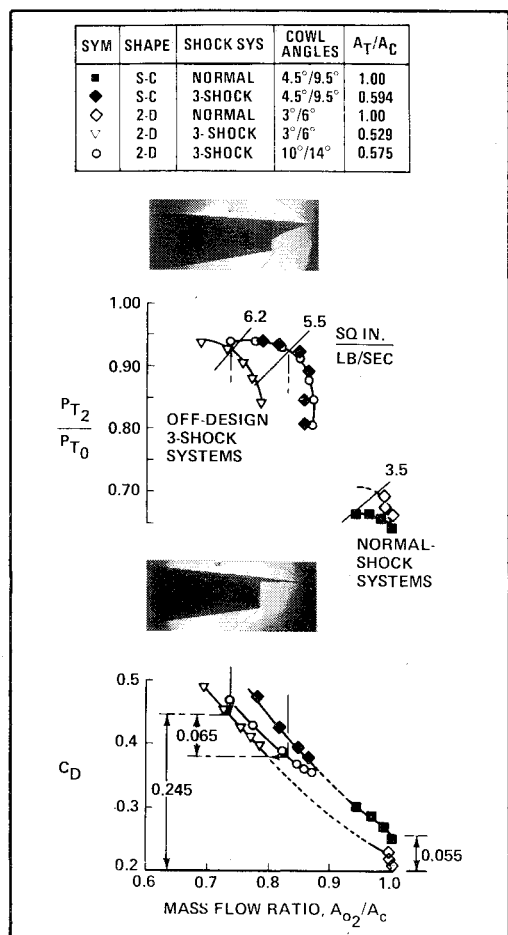


Fig. 6 Off-design shock system.

The inlet model ramps and cones can be translated to change the position of each of the shock waves relative to the lip, in order to investigate shock-lip clearance effects upon stable airflow range and drag.

An alternate configuration for both inlets is a normal shock, minimum cowl angled system for establishing minimum external drag levels. To derive these configurations, the compression surfaces are removed and replaced with flat surfaces having porous area sections for removal of the strong normal-shock/boundary-layer air. The minimum cowl angles are 3/6 deg (internal/external) for the lower cowl lip of the two-dimensional inlet and 4.5/9.5 deg for the semiconical inlet. The semiconical inlet has the larger external angle because of the constraint that the centerlines of the two-dimensional inlet and the engine be identical.

The compression surface boundary-layer control on these models is a bleed removal system comprised of a throat slot and an exit door on the upper surface (see Fig. 4). The bleed slot width is within 35-45% of the throat height for all of the configurations discussed. This geometry was selected because it is within the range over which inlet performance is near optimum and nonvarying, as determined from previous testing. The bleed system exit area and discharge angle, however, can significantly affect inlet operating characteristics, such as maximum mass flow, stable regulation, minimum drag level, and pressure recovery. The sensitivity of these parameters to bleed system exit configuration was investigated.

Discussion of Results

Shock System Comparison

The two normal-shock configurations were compared with their three-shock counterparts. In one case, the three-shock configurations had the minimum external cowl angle used

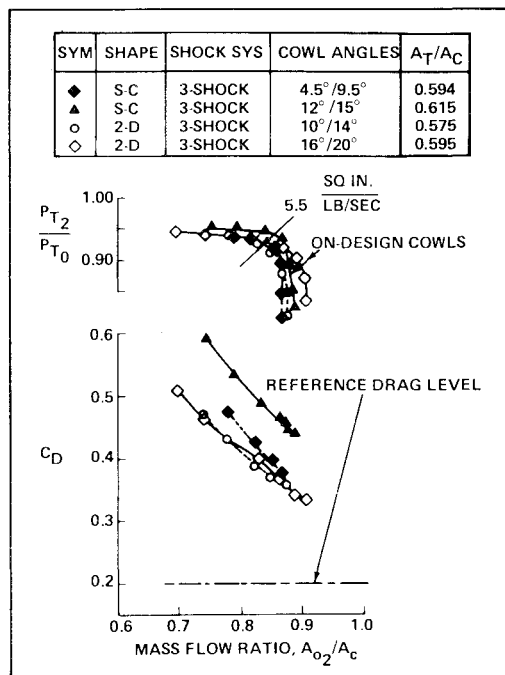


Fig. 7 On-design shock system.

with the normal-shock system, and in another case they had on-design cowl angles to complement the external multishock system.

Figure 6 shows the first case for both semiconical and two-dimensional inlets. The normal-shock comparison shows both inlets choking at the expected mass flow ratio of unity. There is essentially no stable subcritical plateau for the two-dimensional inlet and only a small ($\approx 6\%$) regulation capability for the semiconical inlet. This indicates that the bleed systems are choked and are inadequate to provide a significantly stable airflow range. These bleed systems are, of course, not typical of properly designed normal-shock inlet bleed systems. For our purposes, only an indication of unchoking of the inlet was necessary to determine the critical drag level of each inlet.

The semiconical normal-shock inlet incurs a drag increment of 0.055 C_D above the two-dimensional normal-shock inlet. This value compares very well with the theoretical value of 0.053 C_D , which results from using two-dimensional theory.

When the three-shock compression surfaces were added to the respective two-dimensional and semiconical normal-shock inlets, off-design low cowl angled configurations were created, and the drag penalties for achieving high-pressure recovery were defined (Fig. 6). The mass flow of the two-dimensional inlet is severely reduced, and a matched drag penalty of 0.245 C_D is incurred. This penalty was reduced by 26% by increasing the cowl angles from 3/6 deg to 10/14 deg to provide more throat area, even though the drag characteristic is worsened. An 11% reduction in required capture area is concurrently achieved. The increased throat area of the two-dimensional, three-shock inlet is very close to the throat area of the low cowl angled, semiconical inlet. Therefore, the mass flow vs pressure recovery characteristics of these configurations are very similar, although the two-dimensional inlet's airflow regulation is better.

The drag of the three-shock, semiconical inlet is higher than that of the two-dimensional inlet which provides the same pressure recovery. This is a result of the constraint that the engine and inlet centerlines must be coincidental, leading to a greater external cowl angle for the semiconical inlet. It is significant to note that the drag vs mass flow characteristics of the semiconical configurations (i.e., for both the normal-shock and the three-shock inlets) exhibit virtually identical slopes (Fig. 6).

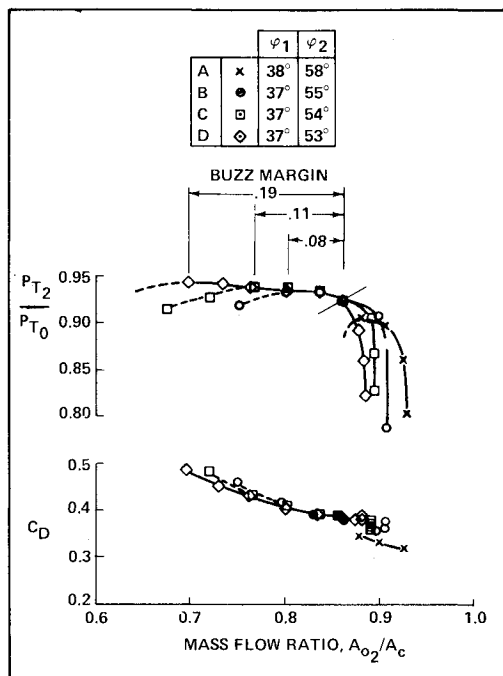


Fig. 8 Oblique shock lip—clearance effects.

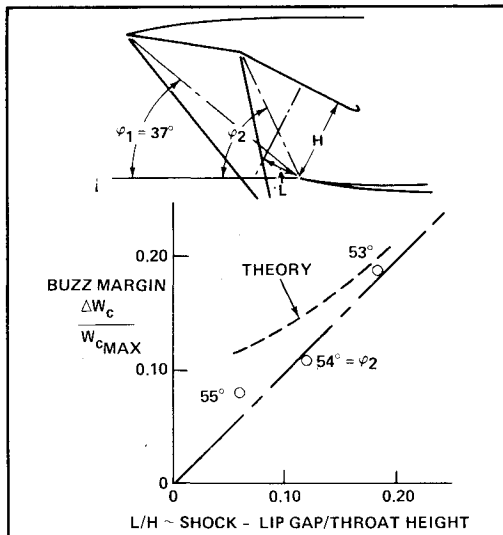


Fig. 9 Oblique shock lip—clearance analysis.

The shadowgraphs show the semiconical inlet operating in a normal-shock configuration, and also as a three-shock configuration after the addition of a biconic compression surface. The single oblique disturbance coming from the leading edge of the normal-shock configuration is a weak one generated by the boundary layer on the overhanging surface. The normal shock is swallowed, and is therefore not seen in the shadowgraph. Although not presented here, shadowgraphs of the two-dimensional normal-shock configuration show a weak oblique shock, which results from boundary-layer displacement effects, entering the inlet. This phenomenon probably explains both the greater pressure recovery and the smaller (actually nonexistent) stable regulation of the two-dimensional inlet relative to the semiconical one, as shown in Fig. 6.

The configurations of Fig. 6 were modified by increasing the cowl angles to their respective design values to provide more throat area and therefore more mass flow (see Fig. 7). The on-design, two-dimensional inlet has a slightly better matched pressure recovery than the off-design configuration, and a small drag penalty. The on-design, semiconical inlet

also has a slightly better matched pressure recovery than its off-design cowl counterpart, but has a matched drag penalty which is 0.05 C_D greater. It is significant that the addition of the greater cowl angles has extended both the maximum and minimum mass flow capability. The 14 and 9.5 deg cowls were increased to 20 and 15 deg, respectively. The greater regulation thus provided bought a much higher drag penalty for the semiconical inlet compared to the two-dimensional inlet.

The apparently greater sensitivity of the semiconical inlet's pressure recovery to cowl lip angle reflects the greater throat periphery. The two-dimensional inlet's cowl lip angle affects only the lower throat wall. For similar reasons, the effects upon external cowl drag follow the same trend, i.e., greater drag reduction for reduced angles on the semiconical inlet.

As for shock-lip clearance, the proximity of the oblique shock waves to the normal shock and the cowl lip is a prime factor in determining the airflow margin available for matching the engine's demand with the inlet's capability. For stability, there should be no intersections between shocks or shock and lip which could result in a slipstream being ingested. Because of its accompanying total pressure deficiency, this can lead to flow reversal and instability upon subsequent diffusion. As inlet airflow is reduced, diffusion increases and the probability of ingestion of a slipstream becomes greater.

A shocks-on-lip design yields the very smallest stable airflow range, but also the least spillage and lowest drag. Other designs can trade spillage drag for improved shock-lip compatibility, i.e., stable airflow range. A study showing the effects of systematically moving the second oblique shock-generating ramp forward to provide greater shock-lip clearance is presented in Fig. 8. Also shown is a configuration having the oblique shocks just 1 deg off the lip (case A).

The relatively low drag of the tightly formed shock system (case A) comes at the cost of poor internal performance. For cases B, C, and D, where the first shock's lip-to-ramp angle is decreased by 1 deg more than case A, better internal performance is obtained at the expense of drag. The loss of throat area accompanying the forward positions of the second ramp causes a near proportional loss of choking mass flow ratio. What is most significant is that the poor regulation capability of case B is substantially improved by the increments in shock-lip clearance of cases C and D. The stable airflow range between the common match point at a mass flow ratio of 0.85 and the buzz point (buzz margin) is improved from 8 to 19%, with no effect upon maximum airflow inlet drag.

It is possible to compare these two-dimensional test results with a theoretical prediction of buzz margin based upon the stability criterion of Ref. 1, i.e., total pressure deficit calculations. Such a comparison is shown in Fig. 9, where a correlation of buzz margin with the ratio of shock-lip gap to throat height works fairly well for the test results. The theoretical estimate overpredicts the buzz margin at low values of gap-to-throat-height ratio, but provides better results at higher values.

This gap-to-throat-height ratio defines the normal-shock position corresponding to the onset of slipstream ingestion. This does not necessarily indicate the onset of buzz; however, it was sufficient for the test case of Fig. 9.

It is possible to get significantly larger buzz margins by employing a lower initial lip-to-ramp angle, thereby allowing more available gap between the second oblique shock and the lip. However, this capability will cost more oblique shock spillage drag. Figure 10 shows the theoretical tradeoff of drag coefficient at the maximum airflow point with buzz margin, corresponding to forward movement of the second ramp. A maximum buzz margin of 35% is shown corresponding to the verge of ingestion of the shock-shock vortex at the maximum airflow point. The drag penalty to provide this benefit is $\Delta C_D \approx 0.10$.

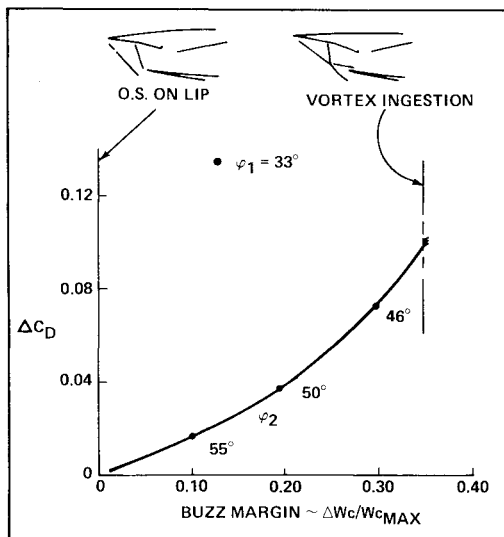


Fig. 10 Oblique spillage vs buzz margin tradeoff.

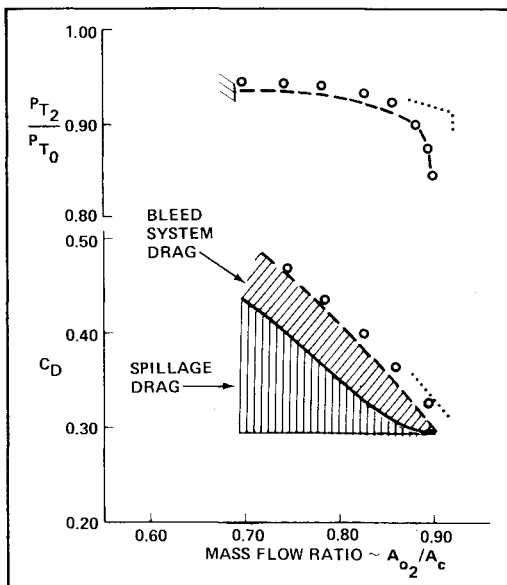


Fig. 11 Comparison of test and theoretical results.

Bleed System Operation

Some insight into the effects of the bleed system operation on the stable airflow range is provided by comparing the test results with theoretical inlet performance. One-dimensional calculations were used to generate the theoretical characteristics in Fig. 11. The agreement with the minimum stable point is very good for this case. The effect of removing the bleed from the theoretical model is seen to be a large reduction in buzz margin, as well as a small migration to higher mass flow ratios. The pseudobypass capability of the throat slot system is responsible for a theoretical buzz margin improvement of from 5% (without) to 21% (with). Of course, the absence of any boundary-layer removal would cause a much poorer performance than that shown for the theoretical case in Fig. 11.

The theoretical contributions of spillage drag and throat slot bleed system drag show that the subcritical slope is largely dictated by the spillage drag effects. The calculation assumes no lip suction variation with mass flow ratio. Notice that at high mass flow ratios the bleed system handles almost all of the subcritical flow, and as mass flow ratio is reduced, the spillage drag becomes a greater contributor to the overall inlet drag. This shows that most of the stable airflow range results

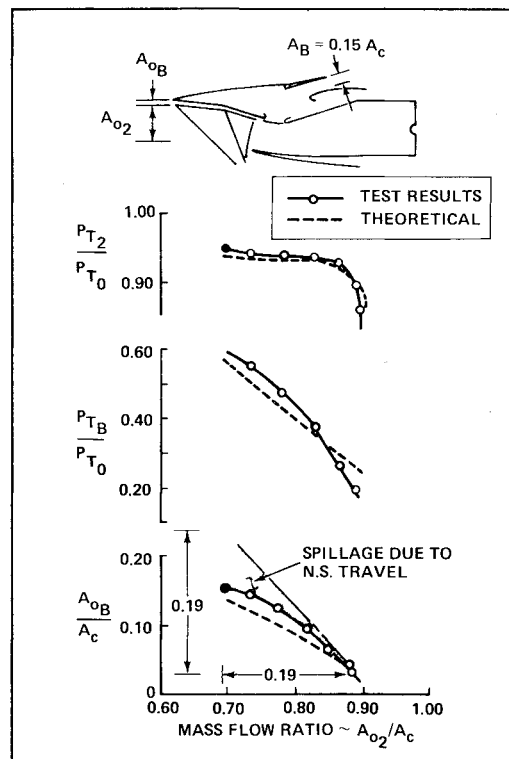


Fig. 12 Bleed system operation.

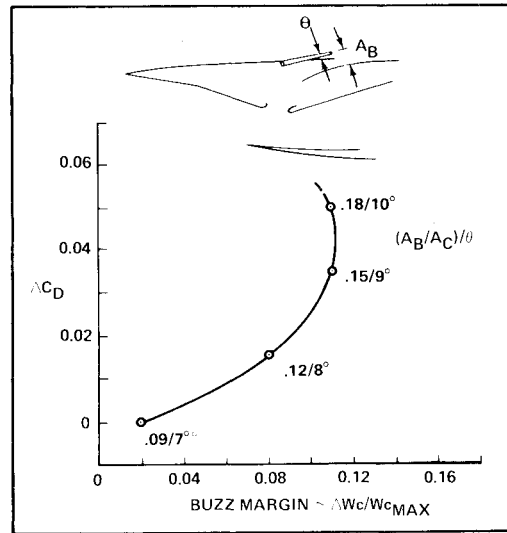


Fig. 13 Using the bleed system as a bypass.

from the bleed system operation. Therefore, investigations of the bleed system test results and theoretical estimates are in order. Bleed exit static and total pressure measurements were used to calculate the bleed flow parameters of Fig. 12.

The bleed exit area, which controls the flow through the bleed system, is unchoked until the throat driving pressure increases to provide about 25% pressure recovery at the bleed exit. Since the bleed system is driven primarily by inlet throat static pressure, the bleed system pressure recovery increases toward lower mass flows where the static pressure is increasing.

At the choked inlet condition, the bleed mass flow ratio is 0.04. This increases to 0.16 at the minimum stable mass flow point. The subcritical bleed flow represents $\approx 63\%$ of the total subcritical (excess) airflow. The remainder of the subcritical mass flow was spilled over the cowl lip as the normal shock moved forward due to the increasing static pressure at the lip.

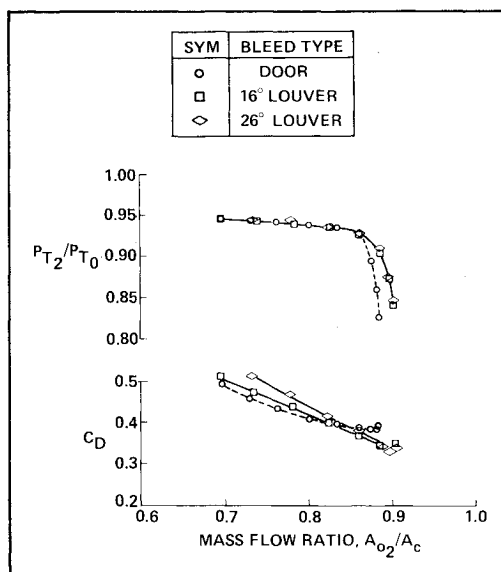


Fig. 14 Bleed exit geometry effects.

This pressure rise stems directly from the decreasing ability of the bleed system to pass flow at low inlet mass flow ratios. The increased lip pressure represents the underlying cause of the onset of inlet instability. Therefore, the effects of increasing the bleed system's flow capacity will be evaluated. However, it is important to note that upstream compression surface bleed, perhaps through a porous section, could improve the slot system's total pressure recovery and, therefore, its mass flow capability.

Bleed System Exit Area

The effects of varying the bleed exit door area from 0.09 to $0.18 A_c$ with a resultant range in discharge angle of 7-10 deg relative to the upstream surface is shown in Fig. 13. The drag increase incurred at the maximum flow point is plotted against the buzz margin for each of the four configurations. This drag is primarily due to the pressure drag on the door, since the momentum drag of the bleed flow is very small. Large benefits in buzz margin are bought with the initial increases in door area. However, there is no improvement in buzz margin as the exit area is increased from 0.15 to $0.18 A_c$. There is approximately a 40% increase in the pressure coefficient acting on the bleed door surface over the range of door positions tested. Therefore, a concurrent increase in the bleed door exit pressure may limit the bleed system flow, thus reducing the system's effectiveness as a bypass device.

Improved bleed system capacity can probably be most effectively provided by longer doors having a smaller angle for the same exit area. Alternatively, a higher pressure recovery in the discharge of the system would allow a greater depression of the buzz point for the same size exit door.

An interesting comparison of the effects of replacing the exit door with louvers having the same geometric area ($0.15 A_c$), but a 16 deg exit angle to the surface instead of the door's 9 deg angle, is shown in Fig. 14. Figure 14 shows the inlet characteristics for the two cases of Fig. 15 as well as for a 26 deg louver configuration.

The two most striking effects are an increase in the choking mass flow and a reduction in choking drag level for both the 16 and 26 deg louvers, with low airflow limits remaining unchanged for the lower angled louver. The more significant of the two effects is the drag change. By eliminating the projected door area, a choked drag reduction was achieved with the louvers at no penalty to internal performance. There is a subcritical drag slope difference, however, with the louvers providing higher slopes. The 16 deg louvers provide the least slope change, while the 26 deg louvers are somewhat higher. A drag reduction of $\approx 0.025 C_D$ for the 16 deg louvers

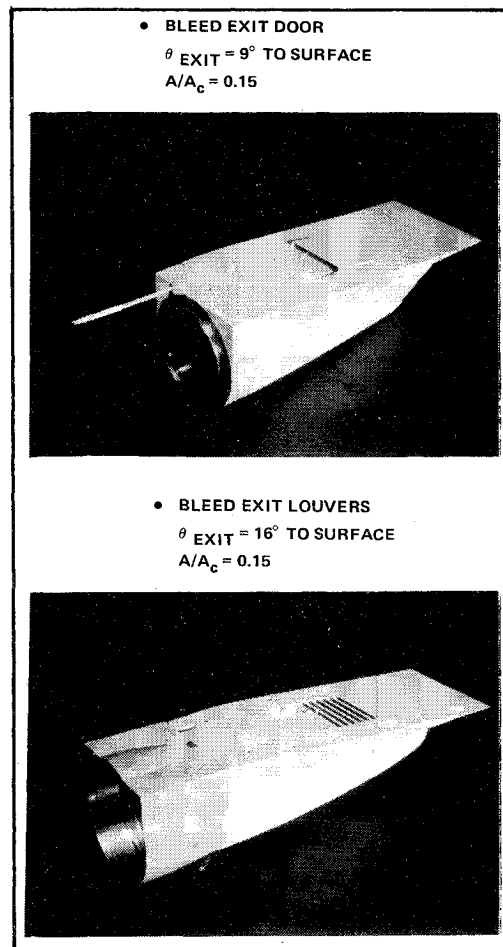


Fig. 15 Bleed exit configurations.

is available for matching engine airflow at 0.86 mass flow ratio. Further high-flow drag improvements, as well as lower subcritical drag, may be possible with lower angled louvers.

Duct Bypass

Although the throat slot boundary-layer removal system can bypass excess air, it is not a true bypass because the inherently low total pressure recovery imposes a relatively small flow capacity. A proper duct bypass was evaluated in the subsonic diffuser section of the two-dimensional model.

The effects of employing a 15 deg bypass door located in the lower duct wall are shown in Fig. 16. The door has an exit area equal to $0.10 A_c$, which translates into 17% of the throat area. The supercritical, or choking, mass flow shift of the performance characteristics correlates well with the 17% of throat area bypassed. The characteristic shape is rounded with somewhat deteriorated performance.

The bypass door provides a substantial drag benefit when compared to the other methods of handling excess airflow. When operating fully open to meet a low engine airflow condition, at a pressure recovery of 0.925, the drag penalty is 60% less than for the door-closed case. In this condition there is still a 10% buzz margin with the door open, compared to no margin with the door closed. If the bypass door is scheduled to open at areas intermediate between closed and full open, then the slope of the resultant drag characteristic is about half of the baseline subcritical drag slope. This is a considerable improvement in the drag penalty for handling excess airflow when compared to shock-lip clearance methods.

Low Mass Flow Ramp Position

An alternative method of increasing the buzz margin is to reduce the inlet throat area by deploying the ramps, the excess

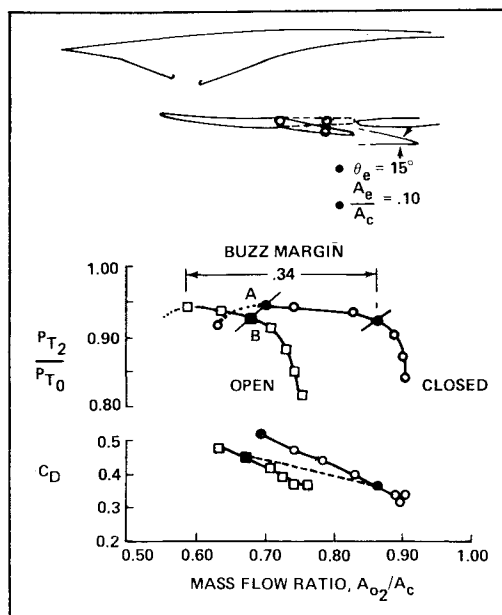


Fig. 16 Bypass door effects.

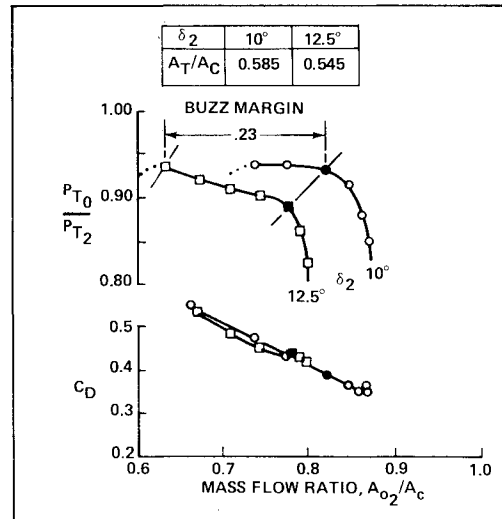


Fig. 17 Ramp deployment effects.

flow being handled by the bleed system as well as through spillage around the cowl lip. This is demonstrated in Fig. 17, where the second ramp is deployed 2.5 deg from the baseline geometry and the aft ramp follows to maintain a baseline bleed entrance. The choking mass flow ratio shift is in direct proportion to the throat area reduction, and the characteristic shape is somewhat deteriorated. However, an improvement to 23% in subcritical stable airflow range is provided. Notice that the drag characteristics are colinear. Therefore, unlike the bypass configuration, they do not provide the low drag benefits at low airflow.

High Mass Flow Ramp Position

Having defined several means of providing adequate buzz margin and the associated drag penalties, it is of interest to evaluate means for reducing the drag at maximum airflow. The most straightforward approach is to operate at high mass flow ratios. Therefore, the ramp turning of $\delta_1/\delta_2 = 10/10$ deg was reduced to $\delta_1/\delta_2 = 10/7$ deg to provide a 10% larger throat area. This approach will dictate a normal-shock Mach number increase from 1.30 to 1.41. The stronger shock/boundary-layer interaction, as well as the smaller shock-to-lip gap resulting from the lower turning angle, will

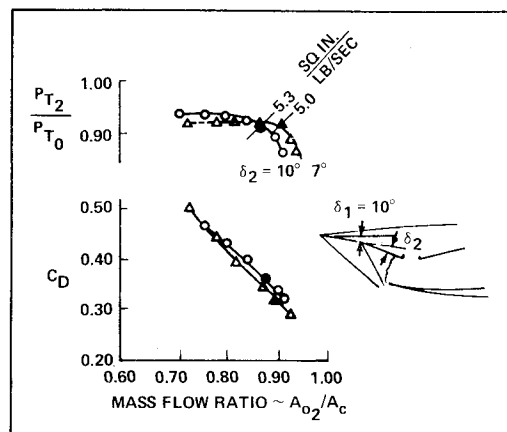


Fig. 18 Ramp turning effects.

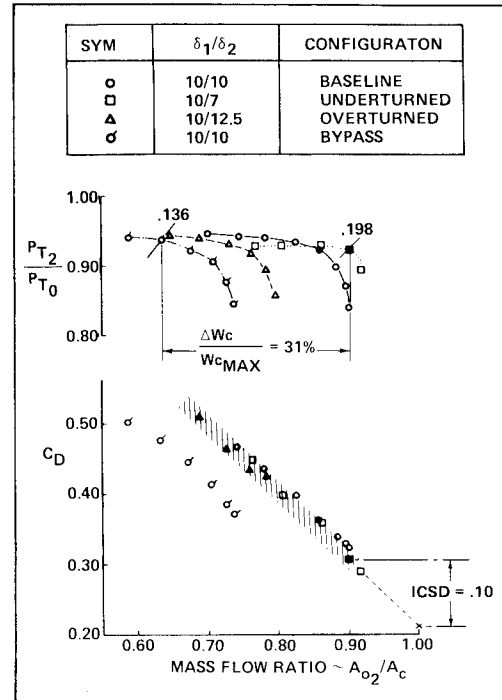


Fig. 19 Inlet performance and matching tradeoffs.

tend to reduce the buzz margin. The results (Fig. 18) show that the usable maximum mass flow ratio for matching a maximum engine requirement has been increased from 0.86 to 0.90, with an attendant 5% reduction in capture area. The concurrent reduction of drag coefficient translates into a 17% improvement in drag. Although the buzz margin appears to be about the same for both configurations in Fig. 18, the portion of the undeturned inlet's subcritical characteristic below a mass flow ratio of 0.76 is metastable. This may be indicative of inadequate boundary-layer removal and/or slipstream ingestion.

These results show that if the technology to extend the maximum usable mass flow ratio into the 90% range were developed, considerable drag improvements could be achieved. In a sense, external compression inlet technology is approaching mixed compression technology.

A comparison of the performance characteristics of several of the configurations studied to evaluate buzz margin and drag characteristics is shown in Fig. 19 to illustrate some important results. The bypass device shows a marked reduction in supercritical drag, but has approximately the same subcritical slope as the other configurations. This mechanism could be applied to any of the other con-

figuration's results to provide increased buzz margin, as well as low subcritical drag. For example, the low drag corresponding to the 0.900 mass flow ratio (darkened) point on the undeturned ramp characteristic could be complemented with a very large buzz margin capability by employing the bypass device.

Many inlet drag bookkeeping methods key on the choked or minimum drag level of the multishock inlet as the reference value. By making a normal-shock version of the inlet the reference configuration, a more realistic assessment of the drag penalty due to the compression system design is provided.

The darkened low drag point is 0.10 C_D above the minimum drag level measured on a normal shock version of the inlet. This increment is due to the inlet's compression system, and is denoted as the inlet compression system drag (ICSD). It represents the total penalty required to provide the increase in pressure recovery above the normal shock level and can be readily measured on complete aircraft models as well as on isolated inlet models.

Conclusions

An experimental investigation was conducted to evaluate the effects of various inlet design elements upon inlet drag and stability. The following conclusions were reached:

1) The lowest drag means for providing large stable airflow regulation was shown to be a bypass device located on a relatively high-pressure recovery duct surface. This device had a 0.10 A_c exit area and demonstrated a buzz margin of 34%. By modulating the door opening, an effective subcritical drag slope of about half the baseline value could be derived.

2) Analysis of the throat bleed slot system indicates that it can serve as a bypass device, although at a greater drag

penalty relative to a dedicated bypass design. It handled 63% of the subcritical excess airflow, the remainder being spilled downstream of the normal shock. This pseudobypass capability is responsible for a theoretical buzz margin improvement of from 5% (without it) to 21%.

3) A louvered bleed exit configuration demonstrated a lower maximum mass flow ratio drag and no compromise in buzz margin, relative to a lower angled bleed exit door of the same physical exit area.

4) A good correlation of buzz margin with the ratio of oblique shock-lip gap to throat height was demonstrated. This parameter defines the normal-shock position corresponding to the onset of slipstream ingestion, but not necessarily the onset of buzz.

5) The ICSD, defined as the difference between matched maximum airflow drag and the minimum value for a normal-shock version of the inlet, has been introduced to provide a more complete approach to quantifying drag characteristics. A minimum ICSD of 0.10 was measured for a two-dimensional inlet operating at a mass flow ratio of 0.90. It is suggested that future inlet design goals should include improving upon this level.

6) The greater sensitivity of the semiconical inlet's performance to the cowl angle, relative to the two-dimensional inlet, leads to a more critical trade between pressure recovery and drag. However, this result could be changed for inlets having different geometry constraints.

Reference

¹Hall, G.R., "A Criterion for Prediction of Airframe Integration Effects on Inlet Stability with Application to Advanced Fighter Aircraft," Paper presented at AGARD Symposium on Airframe/Propulsion Interference, Rome, Italy, Sept. 1974.

From the AIAA Progress in Astronautics and Aeronautics Series

AERODYNAMICS OF BASE COMBUSTION—v. 40

Edited by S.N.B. Murthy and J.R. Osborn, *Purdue University*,
A. W. Barrows and J. R. Ward, *Ballistics Research Laboratories*

It is generally the objective of the designer of a moving vehicle to reduce the base drag—that is, to raise the base pressure to a value as close as possible to the freestream pressure. The most direct and obvious method of achieving this is to shape the body appropriately—for example, through boattailing or by introducing attachments. However, it is not feasible in all cases to make such geometrical changes, and then one may consider the possibility of injecting a fluid into the base region to raise the base pressure. This book is especially devoted to a study of the various aspects of base flow control through injection and combustion in the base region.

The determination of an optimal scheme of injection and combustion for reducing base drag requires an examination of the total flowfield, including the effects of Reynolds number and Mach number, and requires also a knowledge of the burning characteristics of the fuels that may be used for this purpose. The location of injection is also an important parameter, especially when there is combustion. There is engineering interest both in injection through the base and injection upstream of the base corner. Combustion upstream of the base corner is commonly referred to as external combustion. This book deals with both base and external combustion under small and large injection conditions.

The problem of base pressure control through the use of a properly placed combustion source requires background knowledge of both the fluid mechanics of wakes and base flows and the combustion characteristics of high-energy fuels such as powdered metals. The first paper in this volume is an extensive review of the fluid-mechanical literature on wakes and base flows, which may serve as a guide to the reader in his study of this aspect of the base pressure control problem.

522 pp., 6 x 9, illus. \$19.00 Mem. \$35.00 List

TO ORDER WRITE: Publications Dept., AIAA, 1290 Avenue of the Americas, New York, N.Y. 10019